

# Accurate measurement of blood vessel depth in port wine stained human skin *in vivo* using pulsed photothermal radiometry

## Bincheng Li\*

University of California at Irvine  
Beckman Laser Institute and Medical Clinic  
1002 Health Sciences Road East  
Irvine, California 92612

## Boris Majaron

University of California at Irvine  
Beckman Laser Institute and Medical Clinic  
1002 Health Sciences Road East  
Irvine, California 92612  
and  
Jozef Stefan Institute  
Jamova 39  
SI-1000 Ljubljana  
Slovenia

## John A. Viator†

University of California at Irvine  
Beckman Laser Institute and Medical Clinic  
1002 Health Sciences Road East  
Irvine, California 92612

## Thomas E. Milner

University of Texas  
Biomedical Engineering Department  
Austin, Texas 78712

## Zhongping Chen

## Yonghua Zhao‡

## Hongwu Ren

## J. Stuart Nelson

University of California at Irvine  
Beckman Laser Institute and Medical Clinic  
1002 Health Sciences Road East  
Irvine, California 92612  
E-mail: snelson@laser.bli.uci.edu

## 1 Introduction

Successful laser treatment of port wine stain (PWS) birthmarks in human skin is based on selective thermal damage to the targeted blood vessels. The ideal laser treatment should cause irreversible thermal injury to the PWS vessels without injuring the overlying epidermis. Due to melanin absorption, heat produced in the epidermis, if not controlled, may cause serious injury, resulting in permanent complications such as hypertrophic scarring, dyspigmentation, atrophy, or induration. Recently, cryogen spray cooling (CSC) was introduced to cool selectively and protect the epidermis from thermal damage.<sup>1–4</sup> When a cryogen spurt is applied to the skin sur-

**Abstract.** We report on application of pulsed photothermal radiometry (PPTR) to determine the depth of port wine stain (PWS) blood vessels in human skin. When blood vessels are deep in the PWS skin ( $>100\ \mu\text{m}$ ), conventional PPTR depth profiling can be used to determine PWS depth with sufficient accuracy. When blood vessels are close or partially overlap the epidermal melanin layer, a modified PPTR technique using two-wavelength (585 and 600 nm) excitation is a superior method to determine PWS depth. A direct difference approach in which PWS depth is determined from a weighted difference of temperature profiles reconstructed independently from two-wavelength excitation is demonstrated to be appropriate for a wider range of PWS patients with various blood volume fractions, blood vessel sizes, and depth distribution. The most superficial PWS depths determined *in vivo* by PPTR are in good agreement with those measured using optical Doppler tomography (ODT). © 2004 Society of Photo-Optical Instrumentation Engineers. [DOI: 10.1117/1.1784470]

**Keywords:** pulsed photothermal radiometry; photothermal profiling; optical Doppler tomography; port wine stain; two-wavelength excitation.

Paper 03070 received Jun. 2, 2003; revised manuscript received Jan. 30, 2004; accepted for publication Feb. 5, 2004.

face for an appropriate period of time (tens of milliseconds), cooling remains localized in the epidermis while leaving the temperature of deeper PWS blood vessels unchanged. Selective cooling allows subsequent laser heating to raise the PWS temperature above the threshold for permanent blood vessel photocoagulation, while minimizing epidermal injury. The efficacy of CSC depends primarily on selection of the cryogen spurt duration and delay between the spurt and laser pulse. Accurate knowledge of PWS depth on an individual patient basis would provide the necessary information to determine the optimal CSC spurt duration and delay.<sup>4,5</sup>

Pulsed photothermal radiometry (PPTR) is a noncontact method for depth profiling of layered materials.<sup>6,7</sup> PPTR has been used to determine the depth of subsurface chromophores in tissue phantoms and PWS blood vessels in human skin.<sup>8–10</sup> While conventional PPTR using one-wavelength excitation works well for depth determination of deep PWS ( $>100\ \mu\text{m}$ ), the technique fails to resolve blood vessels ly-

\*Current affiliation: Institute of Optics and Electronics, Chinese Academy of Sciences, P. O. Box 350, Shuangliu, Chengdu 610209, China.

†Current affiliation: Oregon Health & Science University, Dept. of Dermatology, OP06 3181 SW Sam Jackson Park Road, Portland, OR 97239.

‡Current affiliation: Carl Zeiss Meditec, Inc, 5160 Hacienda Drive, Dublin, CA 94568.

Address all correspondence to J. Stuart Nelson, University of California/Irvine, Beckman Laser Institute, 1002 Health Sciences Rd E, Irvine, CA 92612, USA. Phone: 949 824 4713; Fax: 949 824 8413; E-mail: snelson@laser.bli.uci.edu

ing in close proximity to the epidermal melanin layer. To overcome this problem, a two-wavelength excitation (TWE) approach was recently introduced to determine the depth of superficial PWS blood vessels.<sup>11</sup> In TWE PPTR, infrared (IR) emission signals following irradiation with respectively 585- and 600-nm laser pulses are recorded sequentially from the same position. Considering that melanin absorption coefficients at 585 and 600 nm are nearly equal, while those of hemoglobin in the blood vessels differ by a factor greater than two, PWS depth can be determined from a weighted difference between the PPTR signals recorded following excitation at these two laser wavelengths.<sup>11</sup>

Determination of PWS depth using the weighted PPTR signal difference is based on a first-order approximation: the PWS temperature profiles induced by 585- and 600-nm laser pulses are nearly proportional. Practically, this approximation depends on the temperature profiles in the PWS layer induced by pulsed irradiation at 585 and 600 nm. These profiles depend on the amount of epidermal melanin, as well as size and spatial distribution of the blood vessels in the dermis, which determine the effective absorption coefficient of the PWS layer.<sup>12,13</sup> Since the blood absorption coefficient at 600 nm is lower than that at 585 nm, 600-nm light penetrates deeper into the PWS layer. Beyond a certain depth, the induced temperature rise at 600 nm may become higher than at 585 nm. If the weighted difference between the induced temperature increases involved in the TWE-PPTR analysis<sup>11</sup> becomes negative, reconstruction of the PWS temperature profile is problematic. To resolve this problem, we propose here an alternative method to determine PWS depth from PPTR signals recorded respectively following laser excitation at 585 and 600 nm.

Outline of this article is: (1) depth determination of deep PWS layers, where we compare the PPTR results with those obtained with optical Doppler tomography (ODT);<sup>14–17</sup> (2) depth determination of shallow PWS layers where we analyze the validity of the first order approximation previously described; and (3) when this approximation is not valid, we present a direct difference analysis method to extract PWS depth and compare the results with those obtained using ODT.

## 2 Theory

PPTR measures the temporal evolution of IR emission from a laser-heated test specimen (e.g., human skin). IR emission signals are then used to reconstruct the depth-resolved temperature distribution immediately after laser irradiation using an inversion algorithm. PWS depth is then determined from the reconstructed depth-resolved temperature distribution. A non-negatively constrained conjugate gradient algorithm was found to be well suited for reconstruction of temperature profiles in laser-heated PWS human skin.<sup>9,18–20</sup>

We assume PWS skin contains an epidermal melanin layer and a single vascular layer in the dermis. The laser spot diameter at the skin surface is assumed to be large relative to the relevant thermal and optical diffusion lengths so that only one-dimensional thermal diffusion along the depth ( $z$ ) axis is considered. Immediately after pulsed laser irradiation, the temperature profile in PWS human skin can be expressed as the sum of the temperature increases in epidermal and PWS layers. At 585-nm excitation, the temperature profile is

$$\Delta T_{585}(z) = \Delta T_{\text{EPI}}(z) + \Delta T_{\text{PWS1}}(z), \quad (1)$$

and the corresponding PPTR signal is, due to linearity of the PPTR signal formation,<sup>19</sup> composed as

$$S_{585}(t) = S_{\text{EPI}}(t) + S_{\text{PWS1}}(t). \quad (2)$$

At 600 nm, we assume that the temperature profile in the epidermis and its corresponding PPTR signal component are approximately equal to that at 585 nm, since the absorption and scattering properties of the epidermis and dermis do not change significantly between the two wavelengths. However, we allow that the temperature profiles in the PWS have different shapes at 585 and 600 nm, because of the complex influence of size and depth distribution on heating of individual blood vessels. We write the temperature profile at 600 nm as:

$$\Delta T_{600}(z) = \beta \Delta T_{\text{EPI}}(z) + \Delta T_{\text{PWS2}}(z), \quad (3)$$

where coefficient  $\beta$  accounts for the small amplitude difference between the epidermal temperature profiles at 585 and 600 nm.<sup>11,21</sup>

By assuming a linear relationship between the two PWS temperature profiles [ $\Delta T_{\text{PWS2}}(z) = \alpha \Delta T_{\text{PWS1}}(z)$ ], they can be determined by eliminating the epidermal contribution to the overall temperature profile:<sup>11</sup>

$$\Delta T_{\text{PWS1}}(z) = \frac{\Delta T_{585}(z) - \Delta T_{600}(z)/\beta}{1 - \alpha/\beta}. \quad (4)$$

For reasons of brevity and clarity, we omit determination of parameter  $\alpha$  and only consider the numerator of Eq. (4),

$$\Delta T_{\text{PWS}}(z) = \Delta T_{585}(z) - \Delta T_{600}(z)/\beta. \quad (5)$$

The weighted temperature difference  $\Delta T_{\text{PWS}}(z)$  in Eq. (5) is proportional to the PWS contribution to the temperature profile at 585 nm, and thus enables determination of the PWS depth (i.e., the top boundary of the PWS layer). This temperature profile can often be reliably reconstructed from the corresponding PPTR signal

$$S_{\text{PWS}}(t) = S_{585}(t) - S_{600}(t)/\beta. \quad (6)$$

When a conjugate gradient inversion algorithm is used, accurate reconstruction of the depth-resolved temperature distribution constrains the solution as non-negative at all depths.<sup>19</sup> From Eq. (5),  $\Delta T_{\text{PWS}}(z)$  may become negative with increasing depth as laser light at 600 nm penetrates deeper into the skin than at 585 nm. When the contribution of negative temperatures from deeper PWS to the weighted PPTR signal difference  $S_{\text{PWS}}(t)$  in Eq. (6) is negligible, PWS depth can be reliably determined. When, however,  $\Delta T_{\text{PWS}}(z)$  becomes negative at a short distance from the most superficial boundary of the PWS layer, reconstruction from the corresponding PPTR signal difference  $S_{\text{PWS}}(t)$  becomes unstable and PWS depth cannot be determined accurately.

The weighted temperature difference can also be obtained by a different method, where the temperature profiles at 585 and 600 nm are independently reconstructed and then used in Eq. (5) to compute  $\Delta T_{\text{PWS}}(z)$ . As in the original approach, optimal value of the parameter  $\beta$  is determined by observing

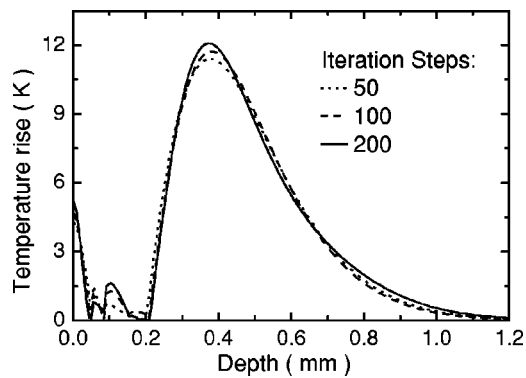


**Fig. 1** Reconstruction of the temperature profile on a PWS site where the epidermal and PWS layers are well separated. The iteration number is 50 (dotted line), 100 (dashed line), and 200 (solid line), respectively.

the profiles  $\Delta T_{\text{PWS}}(z)$  obtained with different  $\beta$ .<sup>11,21</sup> With the optimal  $\beta$ , the epidermal temperature rise minimized, without inducing a negative temperature difference in the epidermal region. In principle, this direct difference method should be applicable to PWS lesions with arbitrary blood vessel size distribution and volume fraction.

### 3 Experimental Methods and Materials

The experimental system used is the same as previously described.<sup>22,23</sup> The ODT apparatus and experimental procedure were described in detail elsewhere.<sup>16,17</sup> Both PPTR and ODT measurements are performed on two PWS patients. The first and second patients have a low (skin type II) and high (skin type IV–V) epidermal melanin concentration, respectively. In PPTR measurements, a PWS site was irradiated with two sequential pulses separated by approximately 1 minute, delivered from a tunable pulsed dye laser (Candela, MA). The first pulse is at 585 nm and the second one at 600 nm. The laser pulse duration is 1.5 ms and the fluence is 6 to 8 J/cm<sup>2</sup>. At this fluence, no significant epidermal damage is observed for both patients. The frame rate of the IR focal plane array camera is 400 or 700 frames per second. For each measurement, 500 frames of IR emission are recorded. Each PPTR signal is determined from approximately 450 to 470 frames recorded after pulsed laser irradiation by subtracting the background level. Each frame is reduced to a single radiometric

temperature by averaging the calibrated IR signals over 64 × 64 pixel region and used as input into the inversion algorithm to reconstruct the initial temperature profile. Details of the reconstruction have been described previously.<sup>9,19</sup>

## 4 Results and Discussions

### 4.1 Deep PWS Layer

A PPTR measurement is first recorded on the hand of a PWS patient where the blood vessels are relatively deep. Figure 1 shows the computed initial temperature profile induced by a laser pulse at 585 nm (pulse duration: 1.5 ms, fluence: 6 J/cm<sup>2</sup>), reconstructed with the non-negative conjugate gradient inversion algorithm and 700-Hz frame rate. Although the maximum temperature of the PWS layer varies slightly when the iteration number is changed from 50 to 200, the reconstruction is stable and PWS depth is determined to be  $\sim 210 \mu\text{m}$ . To verify the PWS depth determined by PPTR, we also measured the same area with ODT. Figures 2(a) and 2(b) show the structural and blood flow velocity images, respectively. The red and blue areas in Fig. 2(b) show respectively, blood flow toward and away from the optical probe. Assuming that the refractive index of human skin is 1.4,<sup>24</sup> the top boundary of the PWS layer is located at a depth of  $\sim 220 \mu\text{m}$ , in agreement with that determined by PPTR. These results demonstrate that depth of deep PWS layers can be accurately determined using the conventional one-wavelength PPTR method. Due to limited ODT signal-to-noise ratio, no PWS blood vessels below 400  $\mu\text{m}$  are observed.

### 4.2 Shallow PWS Layer with Low Blood Volume Fraction

When the PWS layer partially overlaps the epidermal melanin layer, application of the one-wavelength PPTR method is problematic and the two-wavelength approach is applied.<sup>11</sup> Figure 3 shows the results obtained from the arm of a PWS patient with shallow blood vessels. PPTR signals following 585 and 600 nm excitation, respectively, are recorded at a frame rate of 700 Hz. The laser fluence used at both wavelengths is 5 to 6 J/cm<sup>2</sup> and the pulse duration is 1.5 ms. Optimal reconstructions of the corresponding temperature profiles (Fig. 3) are obtained using the non-negatively

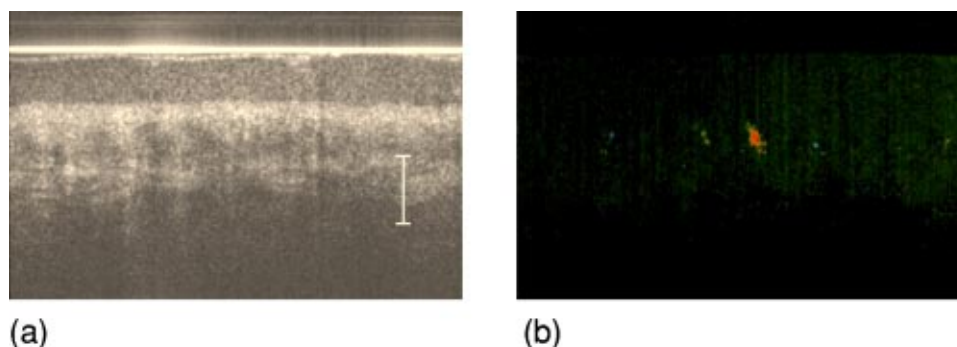


**Fig. 2** ODT images of the same PWS site shown in Fig. 1. (a) Structural image. The top bright line is the glass/skin interface. The scale bar represents 200  $\mu\text{m}$ . (b) Flow velocity image.



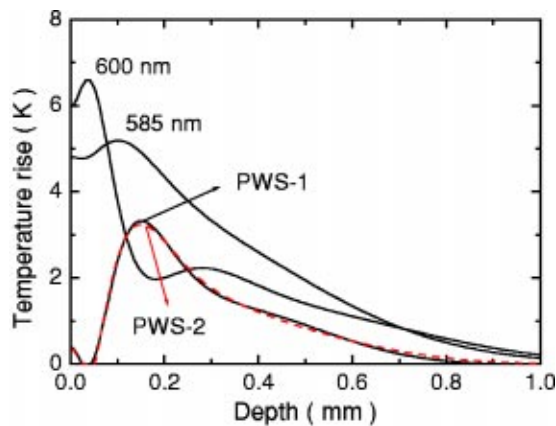


**Fig. 3** Reconstructed temperature profiles on a PWS site where the PWS layer partially overlaps the epidermis (irradiated at 585 and 600 nm), and the weighted difference  $\Delta T_{\text{PWS}}(z)$  (solid line, labeled PWS-1). The iteration number is 5 and 6 at 585 and 600 nm, respectively. The dashed line labeled PWS-2 represents the profile reconstructed from the weighted PPTR signal difference  $S_{\text{PWS}}(t)$ . The iteration number is 200.

constrained conjugate gradient algorithm at iteration numbers 5 and 6, respectively, as determined using the L-curve regularization method.<sup>9</sup>

PWS depth can be determined directly from the reconstructed temperature profiles by using Eq. (5). In this direct difference method, the optimal  $\beta$  value is determined by observing the weighted temperature difference  $\Delta T_{\text{PWS}}(z)$  in Eq. (5) and ensuring that the epidermal temperature rise is minimal and non-negative. The resulting temperature profile ( $\beta^{-1}=0.74$ ) is represented (Fig. 3) by the solid line labeled PWS-1.

Using the original TWE method, the PWS temperature profile is reconstructed from the weighted PPTR signal difference  $S_{\text{PWS}}(t)$  [Eq. (6)]. The optimal solution is determined using the same approach and criterion as above, while also observing the convergence of the iterative reconstruction with different  $\beta$  values.<sup>21</sup> The optimal  $\beta$  and corresponding temperature profile (dashed line labeled “PWS-2” in Fig. 3) are equivalent to that determined with the method described above. The good agreement between results obtained with both methods indicates that both approaches can be used for PWS depth determination ( $\sim 60 \mu\text{m}$ ). In this example, negative temperature difference in  $\Delta T_{\text{PWS}}(z)$  is nonexistent or very small and any adverse effect on  $S_{\text{PWS}}(t)$  is therefore negligible.

#### 4.3 Shallow PWS Layer with High Blood Volume Fraction

In some PWS lesions, a significant negative temperature rise can occur in the weighted temperature difference  $\Delta T_{\text{PWS}}(z)$  [Eq. (5)] at moderate skin depths. Figure 4 shows the temperature profiles at 585 and 600 nm, respectively, reconstructed from measurements on the second PWS patient, as well as the weighted temperature difference obtained by using the direct difference method with optimal  $\beta^{-1}$  value. The applied laser fluence is  $8 \text{ J/cm}^2$ , and the frame rate used to record the PPTR signals is 400 Hz. The maximum PWS temperature at 585 nm is much higher than that of the first patient

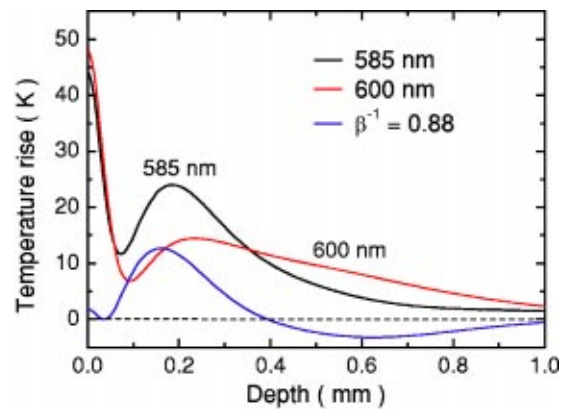


**Fig. 4** Temperature profile reconstructions from another PWS site, where the PWS layer partially overlaps the melanin layer, and the weighted difference with the optimal  $\beta$  value ( $\beta^{-1}=0.88$ ). The iteration step is 30 at 585 and 9 at 600 nm.

(refer to Fig. 3), indicating a high blood volume fraction in this patient’s PWS layer. The 585-nm profile presented in Fig. 4 is obtained with 30 iteration steps, although no significant difference is observed when the iteration number changes from 15 to 40. At 600 nm, the optimal profile is obtained with 9 iteration steps as determined using the L-curve method. The direct difference method can be used to determine a PWS depth of approximately  $60 \mu\text{m}$  (Fig. 4;  $\beta^{-1}=0.88$ ), in good agreement with the value ( $\sim 70 \mu\text{m}$ ) determined from an ODT image (Fig. 5) recorded at the same skin site. The red, blue, and surrounding dark areas show the blood vessels. Compared to Fig. 2, the size of the blood vessels in this patient is larger than those in the first patient, indicating a relatively high overall blood volume fraction.

The previously developed analysis is inappropriate to determine PWS depth of this particular lesion. As seen in Fig. 4, the weighted temperature difference  $\Delta T_{\text{PWS}}(z)$  becomes negative at positions deeper than  $\sim 400 \mu\text{m}$ . The corresponding PPTR signal  $\Delta S_{\text{PWS}}(t)$  is shown in Fig. 6(a) (solid line), and the corresponding reconstructions with different iteration steps are indicated in Fig. 6(b). Due to the influence of the negative temperature at deeper positions of the PWS layer, the reconstruction from corresponding  $\Delta S_{\text{PWS}}(t)$  diverges with increasing iteration number, preventing reliable determination

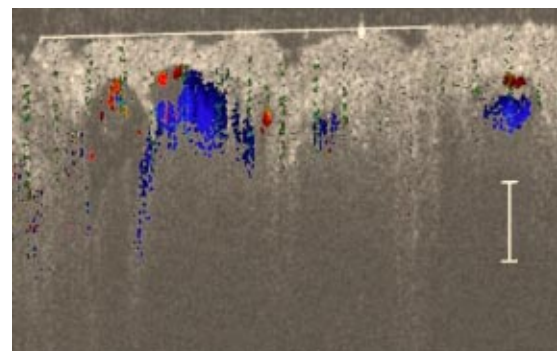


**Fig. 5** ODT image of the same PWS site as in Fig. 4. The white line shows the glass/skin interface. The red, blue, and surrounding dark areas show blood vessels. The scale bar represents  $200 \mu\text{m}$ .

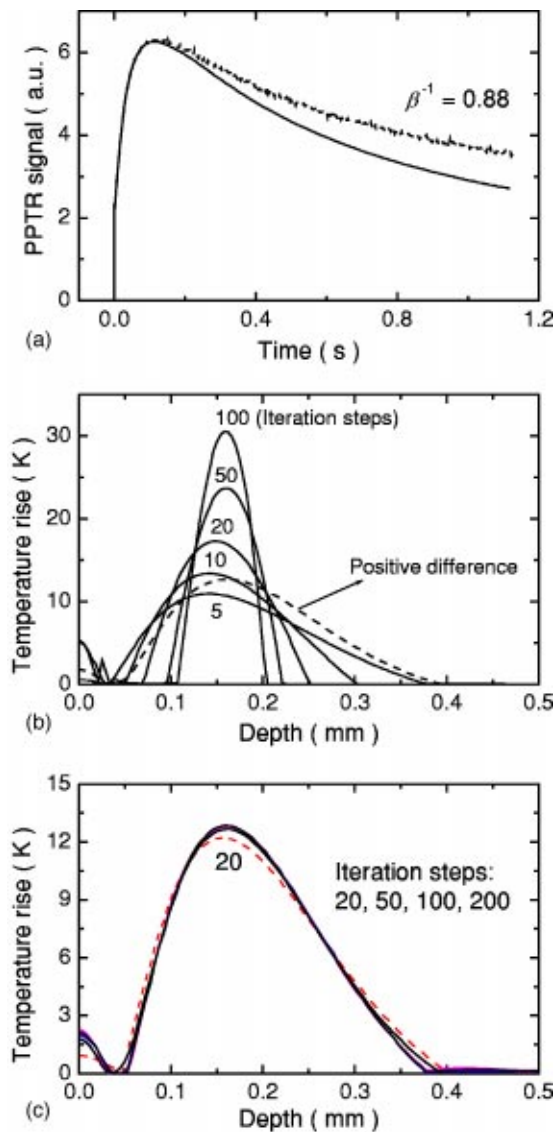


**Fig. 6** (a) Weighted PPTR signal difference  $S_{PWS}(t)$  with  $\beta^{-1}=0.88$  (solid line) and the PPTR signal corresponding to the positive part of  $S_{PWS}(t)$  (dashed line). (b) Reconstructions corresponding to the former  $S_{PWS}(t)$  [the solid line in (a)] with varying iteration steps, showing divergence. (c) Reconstructions corresponding to the PPTR signal shown by the dashed line in (a), showing convergence.

of the PWS depth. To further demonstrate this effect, we calculate the PPTR signal corresponding to the positive part of the temperature difference in Fig. 4 and then reconstruct the temperature profile. The recorded PPTR signal is represented by the dashed line in Fig. 6(a), and the matching reconstructions are presented in Fig. 6(c). With the negative part of the temperature difference eliminated, the reconstruction converges with large iteration numbers.

## 5 Discussion

The results show that when a significant negative temperature difference occurs in  $\Delta T_{PWS}(z)$ , only the direct difference method is appropriate to extract the PWS depth. Validity of the direct difference method is based on precise reconstruction

of the temperature profiles at both wavelengths. The quality of the reconstruction depends essentially on the SNR level of the PPTR signal and the smoothness of the actual profiles. Studies using simulated data show that with sufficient SNR level, a smooth temperature profile can be reconstructed with satisfactory accuracy.<sup>25</sup>

We note the two-wavelength excitation method is also applicable to cases of deep-lying PWS, though in fact it is not necessary since the conventional one-wavelength PPTR method provides sufficient accuracy to determine the PWS depth, as demonstrated in Sec. 4.1.

## 6 Conclusions

We have analyzed the determination of PWS depth *in vivo* using PPTR and compared the results to those determined by ODT. *In situ* measurements on patients show that when the PWS layer lies deep in the skin ( $>0.1$  mm), the conventional one-wavelength PPTR profiling method can be used to determine the PWS depth with sufficient accuracy. When the PWS layer lies in very close proximity to, or partially overlaps, the epidermal melanin layer, PWS depth can be determined by using the two-wavelength excitation approach. Due to the influence of the negative temperature difference on the reconstruction, the previously reported data processing technique, involving reconstruction from a weighted PPTR signal difference, is inappropriate for all PWS lesions with arbitrary blood vessel size distributions and volume fractions. The direct difference approach, utilizing the weighted difference of the temperature profiles reconstructed independently at the two wavelengths, is, in principle, appropriate for any PWS lesion, providing that precise reconstruction of individual temperature profiles is possible. The PWS depths determined using TWE-PPTR are in good agreement with those measured by ODT.

## Acknowledgments

This work was supported by research grants awarded from the National Institutes of Health (EB-2495, AR-47551, AR-48458, HL-64218 and RR-01192), National Science Foundation (BES-86924), and Ministry of Education and Science of the Republic of Slovenia (106-528, SLO-US-2001/19). Institutional support from the Air Force Office of Scientific Research (N00014-94-1-0874), National Institutes of Health, and the Beckman Laser Institute and Medical Clinic Endowment is also acknowledged.

## References

1. J. S. Nelson, T. E. Milner, B. Anvari, B. S. Tanenbaum, S. Kimel, L. O. Svaasand, and S. L. Jacques, "Dynamic epidermal cooling during laser treatment of port-wine stain birthmarks," *Arch. Dermatol.* **131**, 695–700 (1995).
2. B. Anvari, B. S. Tanenbaum, T. E. Milner, S. Kimel, L. O. Svaasand, and J. S. Nelson, "A theoretical study of the thermal response of skin to cryogen spray cooling and pulsed laser irradiation: implications for treatment of port wine stain birthmarks," *Phys. Med. Biol.* **40**, 1451–1465 (1995).
3. H. A. Waldorf, T. S. Alster, K. McMillan, A. N. Kauvar, R. G. Geronemus, and J. S. Nelson, "Effect of dynamic cooling on 585-nm pulsed dye laser treatment of port wine stain birthmarks," *J. Dermatol. Surg.* **23**, 657–662 (1997).
4. J. S. Nelson, B. Majaron, and K. M. Kelly, "Active skin cooling in conjunction with laser dermatologic surgery," *Semin. Cutan. Med. Surg.* **19**, 253–266 (2000).

5. W. Verkruysse, B. Majaron, B. S. Tanenbaum, and J. S. Nelson, "Optimal cryogen spray cooling parameters for pulsed laser treatment of port wine stains," *Lasers Surg. Med.* **27**, 165–170 (2000).
6. A. C. Tam and B. Sullivan, "Remote sensing applications of pulsed photothermal radiometry," *Appl. Phys. Lett.* **43**, 333–335 (1983).
7. F. H. Long, R. R. Anderson, and T. F. Deutsch, "Pulsed photothermal radiometry for depth profiling of layered media," *Appl. Phys. Lett.* **51**, 2087–2089 (1987).
8. S. L. Jacques, J. S. Nelson, W. H. Wright, and T. E. Milner, "Pulsed photothermal radiometry of port-wine-stain lesions," *Appl. Opt.* **32**, 2439–2446 (1993).
9. T. E. Milner, D. J. Smithies, D. M. Goodman, A. Lau, and J. S. Nelson, "Depth determination of chromophores in human skin by pulsed photothermal radiometry," *Appl. Opt.* **35**, 3379–3385 (1996).
10. U. S. Sathyam and S. A. Prahl, "Limitations in measurement of subsurface temperatures using pulsed photothermal radiometry," *J. Biomed. Opt.* **2**, 251–261 (1997).
11. B. Majaron, W. Verkruysse, B. S. Tanenbaum, T. E. Milner, S. A. Telenkov, D. M. Goodman, and J. S. Nelson, "Combining two excitation wavelengths for pulsed photothermal profiling of hypervascular lesions in human skin," *Phys. Med. Biol.* **45**, 1913–1922 (2000).
12. G. W. Lucassen, W. Verkruysse, M. Keijzer, and M. J. C. van Gemert, "Light distribution in a port wine stain containing multiple cylindrical and curved blood vessels," *Lasers Surg. Med.* **18**, 345–357 (1996).
13. W. Verkruysse, G. W. Lucassen, J. F. de Boer, D. J. Smithies, J. S. Nelson, and M. J. C. van Gemert, "Homogeneous versus discrete absorbing structures in turbid media," *Phys. Med. Biol.* **42**, 51–65 (1997).
14. Z. Chen, T. E. Milner, S. Srinivas, X. Wang, A. Malekafzali, M. J. C. van Gemert, and J. S. Nelson, "Noninvasive imaging of in vivo blood flow velocity using optical Doppler tomography," *Opt. Lett.* **22**, 1119–1121 (1997).
15. Z. Chen, Y. Zhao, S. M. Srinivas, J. S. Nelson, N. Prakash, and R. D. Frostig, "Optical Doppler tomography," *IEEE J. Quantum Electron.* **5**, 1134–1142 (1999).
16. Y. Zhao, Z. Chen, C. Saxer, S. Xiang, J. F. de Boer, and J. S. Nelson, "Phase-resolved optical coherence tomography and optical Doppler tomography for imaging blood flow in human skin with fast scanning speed and high velocity sensitivity," *Opt. Lett.* **25**, 114–116 (2000).
17. Y. Zhao, Z. Chen, C. Saxer, Q. Shen, S. Xiang, J. F. de Boer, and J. S. Nelson, "Doppler standard deviation imaging for clinical monitoring of in vivo human skin blood flow," *Opt. Lett.* **25**, 1358–1360 (2000).
18. D. M. Goodman, E. M. Johansson, and T. W. Lawrence, "On applying the conjugate-gradient algorithm to image processing problems," *Multivariate Analysis: Future Directions*, C. R. Rao, Ed., pp. 209–232, North-Holland, Amsterdam (1993).
19. T. E. Milner, D. M. Goodman, B. S. Tanenbaum, and J. S. Nelson, "Depth profiling of laser-heated chromophores in biological tissues by pulsed photothermal radiometry," *J. Opt. Soc. Am. A* **12**, 1479–1488 (1995).
20. D. J. Smithies, T. E. Milner, B. S. Tanenbaum, D. M. Goodman, and J. S. Nelson, "Accuracy of subsurface temperature distributions computed from pulsed photothermal radiometry," *Phys. Med. Biol.* **43**, 2453–2463 (1998).
21. B. Majaron, T. E. Milner, and J. S. Nelson, "Determination of parameter for dual-wavelength pulsed photothermal profiling of human skin," *Rev. Sci. Instrum.* **74**, 387–389 (2003).
22. B. Majaron, W. Verkruysse, B. S. Tanenbaum, T. E. Milner, and J. S. Nelson, "Pulsed photothermal profiling of hypervascular lesions: some recent advances," *Proc. SPIE* **3907**, 114–125 (2000).
23. B. Majaron, W. Verkruysse, B. S. Tanenbaum, T. E. Milner, and J. S. Nelson, "Spectral variation of infrared absorption coefficient in pulsed photothermal profiling of biological samples," *Phys. Med. Biol.* **47**, 1929 (2002).
24. G. J. Tearney, M. E. Brezinski, J. F. Southern, B. E. Bouma, M. R. Hee, and J. G. Fujimoto, "Determination of the refractive index of highly scattering human tissue by optical coherence tomography," *Opt. Lett.* **20**, 2258–2260 (1995).
25. B. Li, B. Majaron, J. Viator, T. E. Milner, and J. S. Nelson, "Performance evaluation of pulsed photothermal profiling of port-wine stain in human skin," *Rev. Sci. Instrum.* **75**, 2048–2055 (2004).